Journal Pre-proof

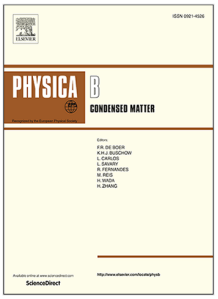

Simulations of optical reflectance in vertically aligned GaAs nanowires array: The effect of the geometrical structural parameters

R.M. de la Cruz, C. Kanyinda-Malu, J.E. Muñoz Santiuste

PII: S0921-4526(22)00284-8
DOI: https://doi.org/10.1016/j.physb.2022.413963
Reference: PHYSB 413963

To appear in: *Physica B: Physics of Condensed Matter*

Received date : 11 November 2021
Revised date : 19 April 2022
Accepted date : 20 April 2022

Please cite this article as: R.M. de la Cruz, C. Kanyinda-Malu and J.E. Muñoz Santiuste, Simulations of optical reflectance in vertically aligned GaAs nanowires array: The effect of the geometrical structural parameters, *Physica B: Physics of Condensed Matter* (2022), doi: https://doi.org/10.1016/j.physb.2022.413963.

Simulations of optical reflectance in vertically aligned GaAs nanowires array: the effect of the geometrical structural parameters

R M de la Cruz[a,1,*], C Kanyinda-Malu[b], J E Muñoz Santiuste[c]

[a] *Departamento de Física, Universidad Carlos III de Madrid, EPS. Avda. de la Universidad 30, 28911 Leganés (Madrid), Spain*

[b] *Departamento de Economía Financiera y Contabilidad II, Area de Matemáticas y Estadística, Universidad Rey Juan Carlos, FCJS, Paseo de los Artilleros s/n, 28032 Madrid, Spain*

[c] *Departamento de Física, Universidad Carlos III de Madrid, EPS. Avda. de la Universidad 30, 28911 Leganés (Madrid), Spain*

Abstract

We report the effects of radius-, length- and pitch-sizes on the optical reflectance of a periodic square array of GaAs nanowires embedded in epoxy. The simulated system is a multilayer array constituted by alternating layers of epoxy and an effective medium of GaAs nanowires embedded in epoxy. For both s- and p-polarizations, we observe an oscillating behavior in the reflectance spectra, as a consequence of interferences in periodical systems. We found that the radius- and pitch-sizes significantly affect the reflectance of GaAs nanowires array, while the length-sizes do not present evidence of changes in the optical reflectance. For higher radius, the number of oscillations increases and consequently, the peak-to-peak distance decreases. Besides, there is a red–shift of the reflectance for increasing radius. For higher pitch, the number of oscillations also increases, and a red–shift is observed. We obtain dependence laws for the peak-to-peak distance and red–shift versus radius and versus pitch. These dependences obey approximate quadratic relations. Attending to the reflectance dependence on the light incidence

*Corresponding author

Email addresses: rmc@fis.uc3m.es (R M de la Cruz), clement.kanyindamalu@urjc.es (C Kanyinda-Malu), jems@fis.uc3m.es (J E Muñoz Santiuste)

[1]Phone: +34 91 624 8733,Fax: +34 91 624 8749

angle, we have found that for s-polarized light, the reflectance is higher with increasing angles, in comparison to p-polarized light cases, independently of the radius and pitch values. For both polarizations, we found that the reflectance is increasing for greater radii and smaller pitchs, independently of the incident angle.

Keywords:
Geometrical effects, Reflectance, GaAs nanowires array, Transfer matrix formalism, Maxwell–Garnett effective model
PACS: 78.20. Bh, 78.20.Ci, 78.55.Cr, 78.67.-n

1. Introduction

Nowadays, the interest on gallium arsenide (GaAs) nanowires (NWs) is continuously increasing by their applications in solar cells [1, 2, 3], nanolasers [4, 5], light emitting diodes [6, 7], field–effect transistors [8], sensors [9] and waveguides [10]. With reference to the application of solar cells, one of the most exciting features of NWs is the geometry dependent absorption characteristics [11, 12, 13, 14, 15, 16], giving them light interaction features not found in a bulk material. In addition, the optical modes on NWs array are strongly dependent on NW diameter, but less dependent on the array pitch and NW length [17]. Dhindsa et al. [18] investigated experimentally and theoretically the absorption and reflectance of ordered vertically GaAs NWs array focusing in their dependence on the diameter and length of the NW and pitch of the array. Azizur-Rahman et al. [19] investigated the optical properties in III-V semiconductor NWs taking into account the influence of geometrical parameters on the absorptance and reflectance. On the other hand, Dhindsa et al. [10] investigated the length dependence on the transmission in silicon (Si) and GaAs NWs array as plausible candidates as waveguides. The above authors performed simulations by using the finite difference time domain (FDTD) method, which takes an extremely long time to calculate. The FDTD method resolves the same equations that the effective medium theories; i.e., Maxwell's eqs., but in a discrete manner, which could entail a study of convergence and accuracy of the method [20, 21]. The effective medium theories are appropriately applied to explain the macroscopic measurements such as the ellipsometry experiments [22, 23]. Recently, we investigated the reflectance dependence of GaAs NWs array on number of bilayers and angle of incidence through the transfer matrix formalism and

effective medium theory for fixed geometrical parameter values [24]. The transfer matrix method has been proven to be very effective for dealing with periodic structures [25] such as the NWs array, being the computing time less than that of the FDTD method.

In this paper, we investigate the geometrical effects on the reflectance of a vertical square array of GaAs NWs. The present study can be useful in the research of photovoltaic solar cells and waveguides applications. The analysis of theses applications is beyond the scope of this work. We use the transfer matrix formalism to analyze the optical reflectance using Fresnel reflectivities within the stacked layers. The array is constituted by alternating layers of islanding material and an effective medium of GaAs NWs embedded in the islanding material. The dielectric function of this effective medium is defined in terms of Maxwell–Garnett (M–G) model [26], where the dielectric function of each NW is described by the Webb formalism [27]. Within this framework, the exciton confinement energy is considered as resonance frequency. This formalism has proven to be successful for low–dimensional systems such as our NWs. In this study, we fix the number of bilayers to 9 to determine the reflectance spectra. This election is motivated for the good approximation obtained in our previous work [24]. The rest of paper is organized as follows. In section 2, we will briefly describe the involved models to calculate the reflectance of square array of GaAs NWs. The implementation of the model in our system along with a discussion of the results are given in section 3. The main remarks and conclusion of this work will be given in section 4.

2. Theoretical model

We investigate the geometrical parameters dependence on the optical properties of a square array of GaAs cylindrical NWs embedded in epoxy, where the epoxy is taken as an example of embedding medium. The array is characterized by cylinder radii ranging between $R = 15\ nm$ to $45\ nm$, length $h = 1000\ nm$ and $2000\ nm$ and array´s periodicity or pitch $a = 100\ nm$, $200\ nm$ and $300\ nm$. These geometrical values are appropriate for the use of effective medium theories and they are approaching to experimental values of NWs grown by conventional techniques [18, 28, 29]. In addition, these geometrical values yield filling factor ($f = \pi(R/a)^2$) belonging to the range between 0.018 to 0.159, which corresponds to a small density of NWs. This small value justifies the use of Maxwell–Garnett effective theory.

To evaluate the optical properties, for the sake of simplicity, we restrict

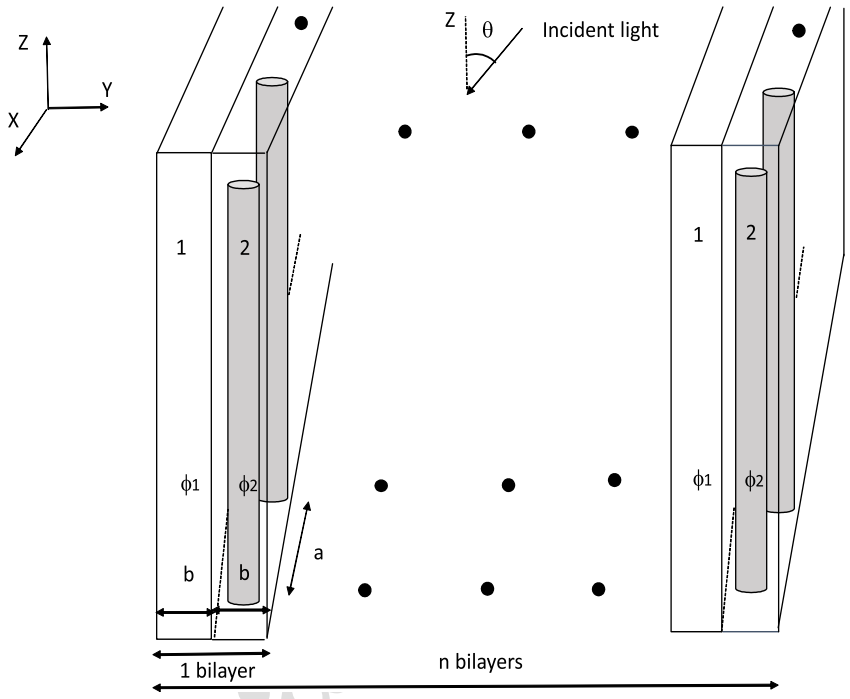

Figure 1: *Scheme of the GaAs NWs array, where z axis is along the NW axis. The multilayer system is constituted by bilayers of epoxy (film 1) and GaAs NWs embedded in epoxy (film 2) of equal thicknesses, being the phase differences for films 1 and 2, ϕ_1 and ϕ_2, respectively.*

our simulations to the system where we have not considered the effect of the substrate. The array is then modeled by a multilayer system composed of 9 periodic bilayers, where each bilayer is constituted by (i) a film of epoxy with dielectric constant ϵ_e and thickness $b = a/2$ and (ii) a film of GaAs NWs embedded in epoxy with an effective dielectric function, which will be discussed later, and with thickness $b = a/2$. This bilayer is periodically distributed in the space up to 9 periods. In a previous paper, we demonstrated that the election of up to 9 bilayers is a good approach to get the main features of optical reflectance in multilayer systems [24]. Figure 1 depicts the scheme of the multilayer system, where we indicate the direction of the incident light. We implement the numerical simulations over the wavelength range 300 nm to 1100 nm which cover the relevant parts of solar spectrum. Then, the wavelength of incident light is larger than the NWs diameter and the light sees the whole assembly as an effective medium; therefore, the use of M–G theory is a good approach in the simulations.

The reflectance spectrum of the NWs array is calculated using the Fresnel expressions for multilayer system, but before doing that it is necessary to characterize the dielectric function of a bilayer constituted by layers 1 and 2 (see fig. 1). The layer 1 is epoxy, an isotropic material with dielectric constant $\epsilon_1 = \epsilon_e = 3$, while layer 2 is an effective medium constituted by GaAs NWs embedded in epoxy, where $\epsilon_2^{||}(\omega)$ and $\epsilon_2^{\perp}(\omega)$ are the effective dielectric functions in the directions parallel and perpendicular to the axis of cylindrical NWs. For modeling the electromagnetic response of a GaAs NWs array, we use the Maxwell-Garnett model with a small density of NWs [26, 30]. Therefore, the effective permittivity of the layer 2 in the direction parallel to the cylinder axis, $\epsilon_2^{||}(\omega)$, can be written as [30, 31]

$$\epsilon_2^{||}(\omega) = f\epsilon_{NW}(\omega) + (1-f)\epsilon_e \tag{1}$$

where f is the filling factor and $\epsilon_{NW}(\omega)$ is the GaAs NW dielectric function that we will describe later. On the other hand, the permittivity of the effective medium in the direction perpendicular to the cylinder axis, $\epsilon_2^{\perp}(\omega)$, can be written as [30, 31]

$$\epsilon_2^{\perp}(\omega) = \epsilon_e \left(\frac{\epsilon_{NW}(1+f) + \epsilon_e(1-f)}{\epsilon_{NW}(1-f) + \epsilon_e(1+f)} \right). \tag{2}$$

We will describe the dielectric function of GaAs NWs by using the formalism

of Webb et al. [27] which is appropriate for low–dimensional systems, i.e.,

$$\epsilon_{NW}(\omega) = \epsilon_\infty + \frac{8e^2}{V\epsilon_o m_{ex}}\left[\frac{2\rho - 1}{\omega_{ex}^2 - \omega^2 - i2\omega\gamma}\right]. \quad (3)$$

The above parameters ϵ_∞, e, ϵ_o, m_{ex}, V, ρ and ω_{ex} are extensively defined elsewhere [27, 24]. In fact, $\rho > 0.5$ provides a lossy resonance (absorption) and $\rho < 0.5$ gain. We neglect the thermally excited electrons, then we assume $\rho = 1$ for lossy resonance. In addition, the approximate exciton energy ($E_{ex} = h\omega_{ex}$) is taken as

$$E_{ex} = E_g + \frac{\hbar^2\chi_{0,1}^2}{2m_e^* R^2} + \frac{\hbar^2\pi^2}{2m_e^* h^2} + E(Coulomb) \quad (4)$$

where $E_g = 1.424\ eV$ ($= 870\ nm$) is the intrinsic GaAs band gap energy, the second and third terms describe the kinetic energy of the exciton in the perpendicular and parallel directions to the NW axis, respectively [24] and the last term is the exciton Coulomb interaction, which represents the exciton binding energy. For the Wannier excitons in semiconductors, this binding energy is small. In fact, the approximate value of the Coulomb term is around -7.7×10^{-3} eV [32], which is negligible compared with the other three terms. In addition, this value could only affect the far infrared spectrum, region which is not of our interest. Hereafter, this term will not be taken into account to evaluate the exciton energy.

With the knowledge of dielectric permittivity of each layer composing the bilayer, the characteristic matrix of a bilayer is given by [33]

$$\mathrm{M}=\frac{1}{1-r_{12}^2}\begin{pmatrix} e^{-i(\phi_1+\phi_2)} - r_{12}^2 e^{-i(\phi_1-\phi_2)} & r_{12}(e^{i(\phi_1+\phi_2)} - e^{i(\phi_1-\phi_2)}) \\ r_{12}(e^{-i(\phi_1+\phi_2)} - e^{-i(\phi_1-\phi_2)}) & e^{i(\phi_1+\phi_2)} - r_{12}^2 e^{i(\phi_1-\phi_2)} \end{pmatrix} (5)$$

where r_{12} is the reflection coefficient at the 1/2 interface and ϕ_1 and ϕ_2 are the phase differences of layers 1 and 2, respectively (see figure 1). Then, the light getting trough 9 periodic bilayers will be defined by M^9. The overall reflection coefficient from the multilayer system is then given by $r = M_{21}/M_{11}$, where M_{21} and M_{11} are the elements of the final transfer matrix (M^9) [33]. This theoretical approach thus allow us to calculate the reflectance for s- and p-polarizations, $R^{(s,p)}$, from the NWs array in form of $R^{(s,p)} = |r^{s,p}|^2$. Herein, the superscripts s and p refer to the s- and p-polarizations, respectively. Then, the expression of coefficient $r^{(s,p)}$ depends of the number of

repeated bilayers considered in the study. In fact, for $n = 9$, its expression is huge and complicated; therefore, we only describe the mathematical expression of M_{21} and M_{11} for 3 bilayers as an example; i.e.,

$$\begin{aligned} M_{21} &= \frac{1}{(1-r_{12}^2)^3}[(e^{-i(\phi_1+\phi_2)} - e^{-i(\phi_1-\phi_2)}r_{12}^2) \\ &\times ((-e^{-i(\phi_1-\phi_2)} + e^{-i(\phi_1+\phi_2)})r_{12}(e^{-i(\phi_1+\phi_2)} - e^{-i(\phi_1-\phi_2)}r_{12}^2) \\ &+ (-e^{-i(\phi_1-\phi_2)} + e^{-i(\phi_1+\phi_2)})r_{12}(e^{i(\phi_1+\phi_2)} - e^{i(\phi_1-\phi_2)}r_{12}^2)) \\ &+ (-e^{-i(\phi_1-\phi_2)} + e^{-i(\phi_1+\phi_2)})r_{12}((-e^{-i(\phi_1-\phi_2)} + e^{-i(\phi_1+\phi_2)}) \\ &\times (e^{-i(\phi_1-\phi_2)} + e^{i(\phi_1+\phi_2)})r_{12}^2 + (e^{i(\phi_1+\phi_2)} - e^{i(\phi_1-\phi_2)}r_{12}^2)^2)] \end{aligned} \tag{6}$$

and

$$\begin{aligned} M_{11} &= \frac{1}{(1-r_{12}^2)^3}[(e^{-i(\phi_1+\phi_2)} - e^{-i(\phi_1-\phi_2)}r_{12}^2) \\ &\times ((-e^{-i(\phi_1-\phi_2)} + e^{-i(\phi_1+\phi_2)})(-e^{i(\phi_1-\phi_2)} + e^{i(\phi_1+\phi_2)}r_{12}^2) \\ &+ (e^{-i(\phi_1+\phi_2)} - e^{-i(\phi_1-\phi_2)})r_{12}^2)^2 + (-e^{i(\phi_1-\phi_2)} + e^{i(\phi_1+\phi_2)})r_{12} \\ &\times (e^{i(\phi_1+\phi_2)} - e^{i(\phi_1-\phi_2)})r_{12}^2)] \end{aligned} \tag{7}$$

where

$$r_{12}^s = \frac{k_1^{||}(\omega) - k_2^{||}(\omega)}{k_1^{||}(\omega) + k_2^{||}} \tag{8}$$

is the reflection coefficient at the interface 1/2 for s-polarization and

$$r_{12}^p = \frac{\epsilon_1^{||}(\omega)k_2^{\perp}(\omega) - \epsilon_2^{||}(\omega)k_1^{\perp}(\omega)}{\epsilon_1^{||}(\omega)k_2^{\perp}(\omega) + \epsilon_2^{||}(\omega)k_1^{\perp}(\omega)} \tag{9}$$

the corresponding for p-polarization [34]. In the above eqs., the superscripts $(||)$ and $(\perp)$ refer to the parallel and perpendicular directions to the axis of the cylindrical NWs.
The wave vectors and dielectric functions in the above equations are reported elsewhere [34, 24]; i.e.,

$$k_1^{||}(\omega) = k_1^{\perp}(\omega) = \frac{\omega}{c}\sqrt{\epsilon_1}cos\theta, \tag{10}$$

where θ is the angle of incident light (see figure 1) and c the speed of light;

$$k_2^{||}(\omega) = \frac{\omega}{c}\sqrt{\epsilon_2^{||}(\omega) - \epsilon_1 sin^2\theta}, \tag{11}$$

and

$$k_2^{\perp}(\omega) = \frac{\omega}{c}\sqrt{\frac{\epsilon_2^{||}(\omega)}{\epsilon_2^{\perp}(\omega)}}\sqrt{\epsilon_2^{\perp}(\omega) - \epsilon_1 sin^2\theta}. \tag{12}$$

Finally, the phase differences ϕ_1 and ϕ_2, appearing in eq. 5 and fig. 1, are defined by $\phi_1 = k_1^{||}.b$ and $\phi_2 = k_2^{||}.b$ or $\phi_2 = k_2^{\perp}.b$ for s- or p-polarization, respectively. When $\theta = 0^o$, $k_2^{||} = k_2^{\perp}$ and consequently, the phase difference ϕ_2 is the same for s- and p-polarization.

3. Results and discussion

The simulated GaAs NWs array has been schematically described in figure 1. The effects of the geometrical structural parameters on the reflectance of this array is discussed in terms of the transfer matrix for 9 bilayers since this number of bilayers is large enough to obtain the main features of the system optical reflectance [24]. Indeed, 9 bilayers is equivalent to 18 single alternated GaAs NW -epoxy layers, that is enough to converge to acceptable result as it was discussed previously in reference [24]. The geometrical parameter values investigated belong to the validity range of the M–G theory. We follow the standard definition of s- and p-polarized light [33]. To clarify the presentation of our results, we divide the discussion in three subsections, accounting for the geometry structural effects of the radius, length and pitch on the reflectance array.

3.1. Radius effect on GaAs NWs reflectance

We show in figure 2 (a and b) the reflectance of the system for different cylinder's radii, with fixed pitch $a = 200\ nm$ and length $h = 1000\ nm$ for s- and p-polarized light when the incident angle is $\theta = 0^o$. We obtain an identical oscillating behavior of the reflectance on the geometrical parameters for both light polarizations (see figure 2). Sikdar and Kornyshev [34] have shown that for the normal incidence, reflectance spectra undergo identical reflection both for s- and p-polarized light for nanoparticle layers. In addition, as we

commented in section 2, when $\theta = 0^o$, $k_2^{||} = k_2^{\perp}$ and consequently, the phase difference ϕ_2 is the same for s- and p-polarization. This characteristic is exactly similar to that previously obtained for other cylinder's geometrical values of GaAs NWs [24].

The obtained oscillating behavior is consistent with the periodicity of the system. In fact, such behavior is extensively reported for the reflectance in different periodical systems [35, 36, 37, 38, 39, 40]. The effects of interference in periodical systems yield oscillations in their reflectance [29]. As white light impinges on the NWs, photons can interact with NWs and undergo multiple scattering, yielding interference effects due to relative phase difference between reflected waves. For both models, continuum M–G theory [29] and discrete FDTD method [18, 29], the oscillating behavior in the optical spectra of III-V NWs assembly is obtained. In fact, Floris et al. [29] used M–G and FDTD models obtaining for the optical reflectance of InAs NWs array a large modulation that depends on the polarization, wavelength and incidence angle of the radiation. Therefore, the above simulated results in InAs NWs array support our simulations in GaAs NWs array with effective theory.

When the cylinder's radius increases, our simulations for both s- and p-polarization demonstrate that: (i) the number of oscillations increases and consequently, the peak-to-peak separation decreases; (ii) the oscillations maxima peak are red–shifted and (iii) the reflectance values are higher. A greater cylinder's radius implies a bigger area of the scattering centers, which entails a higher number of oscillations and consequently, smaller distance between oscillation maxima. We obtain an approximate law for the peak-to-peak distance as (1.27 - $2.6\times10^{-4}R$ - $5.2\times10^{-5}R^2$) where R is the cylinder's radius. Dhindsa et al. [18] reported for experimental and simulated reflectance by FDTD method in GaAs NWs array a red–shift for increasing diameter of the cylindrical NWs, which support our simulations with M–G theory. In fact, for the red–shift oscillations, we obtain a quadratic dependence of the simulated reflectance with the radius–size (3.18 - 0.003 R - $8.2\times10^{-5}R^2$). These results are consistent with those previously reported for absorptance and reflectance in GaAs and InAs NWs [18, 41, 42].

We show in figure 3 (a and b) the reflectance for different cylinder's radii, with fixed pitch $a = 200$ nm and length $h = 1000$ nm for s- and p-polarized light when the incident angle is $\theta = 30^o$. The reflectance values

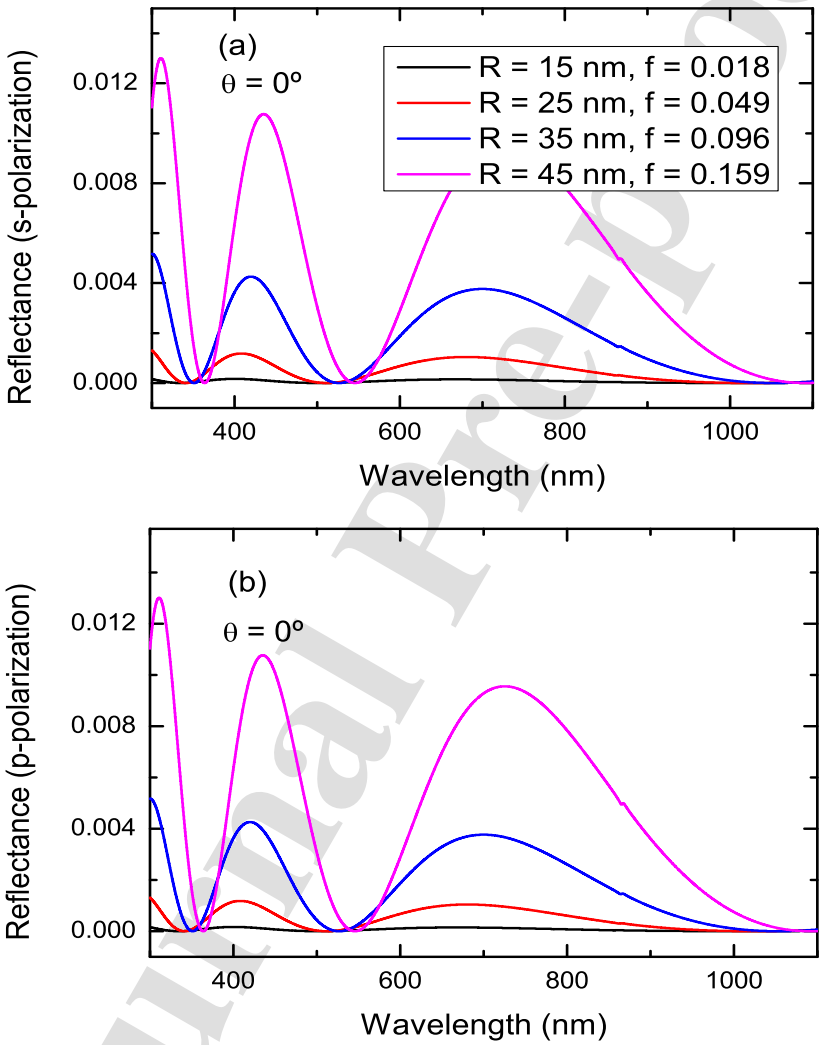

Figure 2: *Reflectance for s- (a) and p- (b) polarized light of the GaAs NWs for angle of incidence $\theta = 0^o$ and different cylinder's radius. The pitch of the array is $a = 200$ nm and the length of NWs is $h = 1000$ nm. The color's code is the same for figures (a) and (b).*

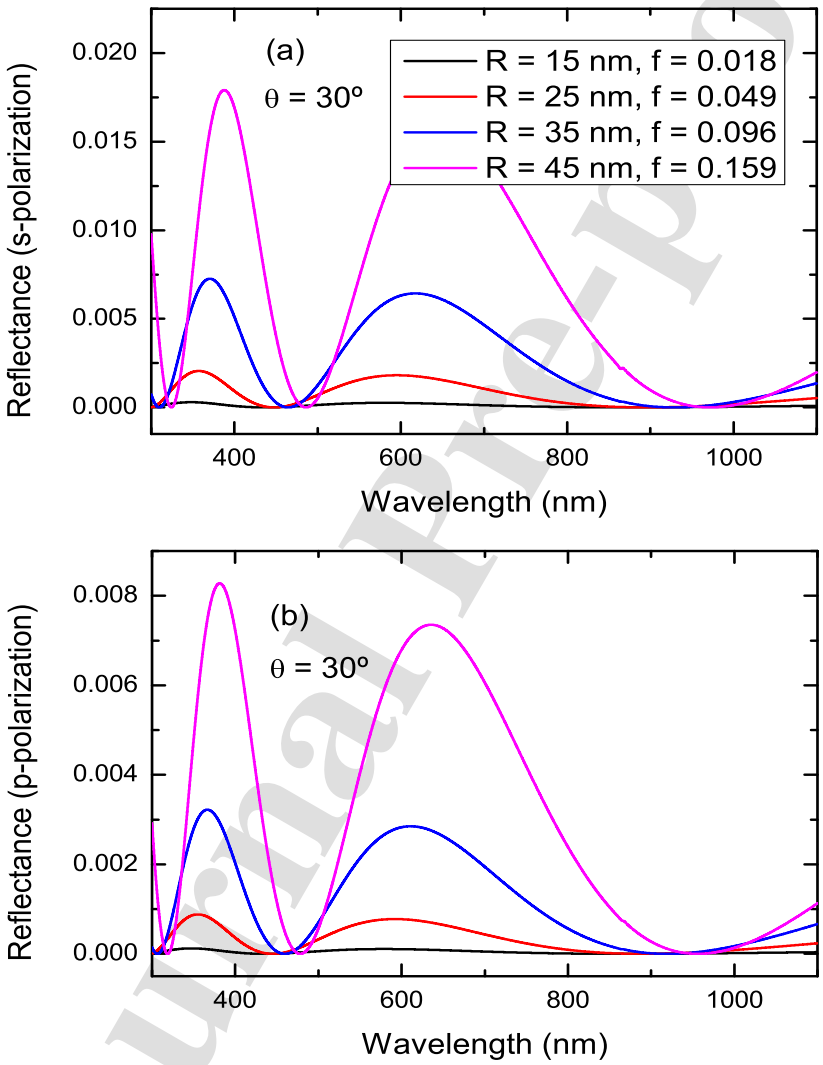

Figure 3: *Reflectance for s- (a) and p- (b) polarized light of the GaAs NWs array with a = 200 nm, h = 1000 nm and different radii. The angle of incidence is θ = 30° for both polarizations. The color's code is the same for figures (a) and (b).*

for s-polarization are higher than for those of p-polarization, independently of the radius investigated. This characteristic reveals that the p-polarization seems to be a better scheme than the s-polarization for oblique incidence to reduce reflectance. In addition, the number of oscillations decreases for both polarizations compared with the case of normal incidence; then, the peak-to-peak distance increases. We obtain approximate laws for peak-to-peak distance as ($1.44 + 8.0\times10^{-5}R$ - $8.5\times10^{-5}R^2$) for s-polarization and ($1.43 + 0.002\ R$ - $1.1\times10^{-4}R^2$) for p-polarization. When the incident angle is higher, the light detects less scattering centers (GaAs NWs) and consequently, the number of oscillations is smaller. This phenomenon was previously reported for other geometrical parameter values of GaAs NWs [24]. For $\theta = 30^o$, we observe red–shift oscillations. The relationship of the maxima peak position with R is ($3.59 + 5.8\ \times10^{-4}R$ - $2.1\times10^{-4}R^2$) for s-polarization and ($3.66 - 0.002\ R$ - $1.52\times10^{-4}R^2$) for p-polarization. Therefore, the dependence laws of peak-to-peak distance and red–shift with the radius are slightly different for s- and p-polarization at oblique incidence. Although it is not shown here, the reflectance dependence on radius for higher angles of oblique incidence follows a similar tendency to that obtained for $\theta = 30^o$. In fact, for increasing angles, the reflectance values for s-polarization are higher than those of p-polarization, as reported in other periodical systems [29, 43].

To summarize and in order to emphasize the above laws with the radius of the NWs, we show in figures 4 (a and b) and 5 (a and b) the dependences of peak-to-peak distance and red–shift with R for s- and p-polarized light, respectively.

3.2. Length effect on GaAs NWs reflectance

Other geometrical parameter we analyze is the NW length. Figure 6 (a, b, c and d) shows the reflectance of s-polarization for cylinder's lengths of $h = 1000\ nm$ and $2000\ nm$ with four different cylinder's radius and pitch $a = 200\ nm$ at normal incidence. Surprisingly, our simulations show identical reflectance values for the two investigated lengths, independently of the radii values (see figure 6). Some authors demonstrated that the reflectance does not change with the length of the NWs in the center wavelength region [18]. In fact, Anttu et al. [42] reported that the simulated reflectance of InP NWs array is constant with the NW length in the interval from $1000\ nm$ to $6000\ nm$. For $R = 15\ nm$ and $25\ nm$ (see figures 6a and 6b), we obtain a feature peaked at $850\ nm$, similar to that reported in GaAs NWs for small radii [24], which is ascribed to GaAs band gap energy. Although it is not shown here,

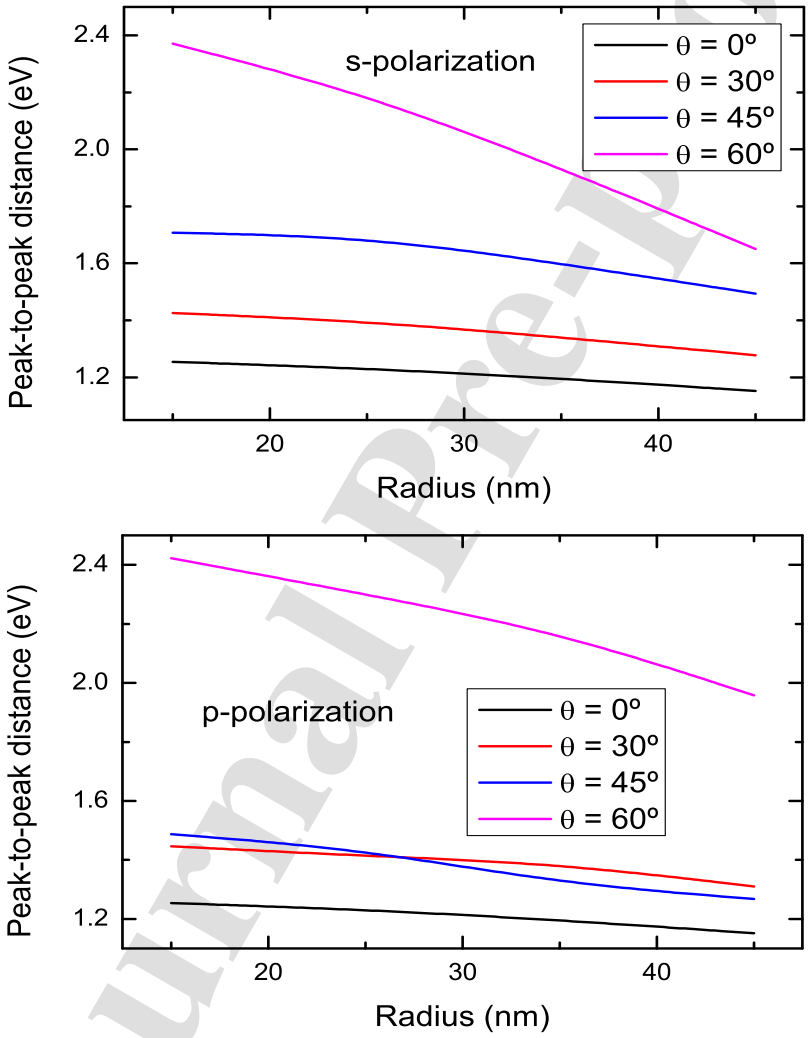

Figure 4: *Peak-to-peak distance versus radius for s- (a) and p- (b) polarized light with angles of incidence $\theta = 0^o$, 30^o, 45^o and 60^o. The pitch of the array is $a = 200$ nm and the length of the NWs is $h = 1000$ nm.*

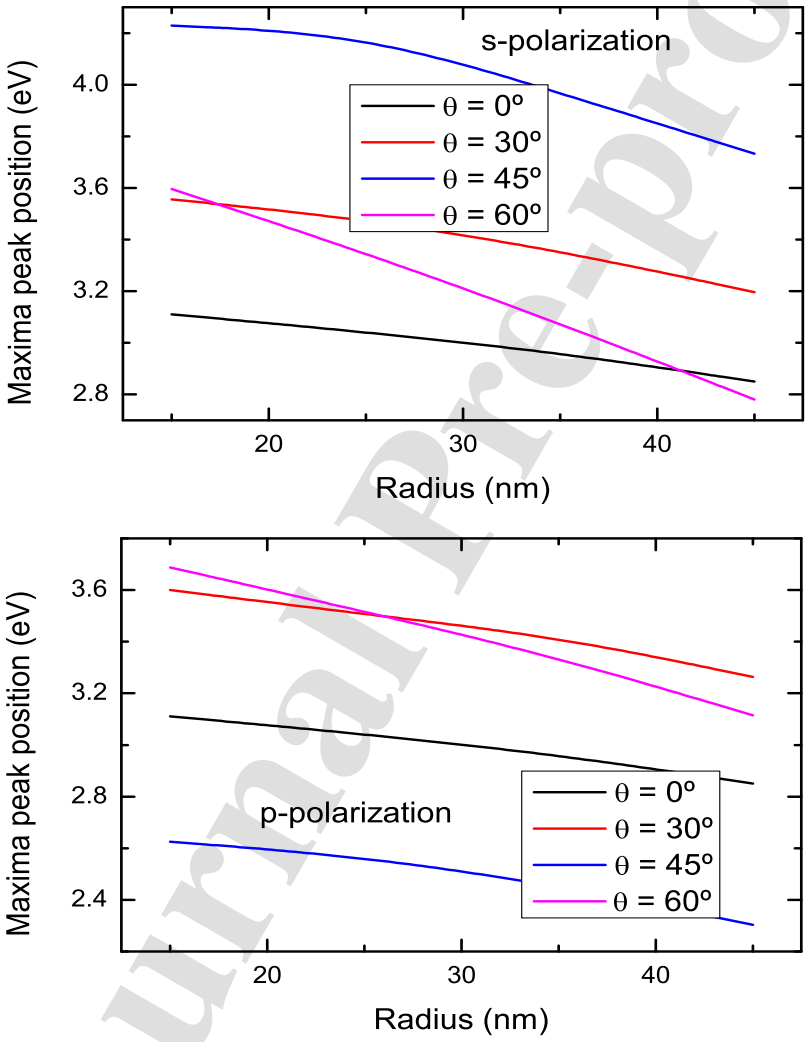

Figure 5: *Maxima peak position (red-shift) versus radius for s- (a) and p- (b) polarized light with angles of incidence $\theta = 0^o$, 30^o, 45^o and 60^o. The pitch of the array is $a = 200$ nm and the length of the NWs is $h = 1000$ nm.*

for oblique incidence, we obtain again that the NW length does not affect the reflectance.

3.3. Pitch effect on GaAs NWs reflectance

Some authors [44] showed that when the light wavelength is of the same order of magnitude as the array's pitch, the light trapping in the NW is more efficient. Then, this geometrical parameter is relevant on the reflectance spectra. Figure 7 (a and b) depicts the reflectance of s-polarization for array's pitch of $a = 100\ nm$, $200\ nm$ and $300\ nm$ with two different cylinder's radii. We obtain for the two investigated radii that the reflectance values are higher when the array pitch is smaller. Also, the number of oscillations increases for greater pitch. We obtain an approximate law for the peak-to-peak distance versus pitch a as (4.34 - 0.02 a + $4.04\times10^{-5}a^2$) for $R = 15$ nm. In addition, our simulations also show a red–shift of the maxima peak position with increasing pitch. We obtain an approximate law as (4.42 - 0.01 a + $1.69\times10^{-5}a^2$) for $R = 15\ nm$.

In figure 7, it is shown that the reflectance values for $R = 25\ nm$ are 7 times higher than the reflectance values for $R = 15\ nm$. On the other hand, for both radii and $a = 100\ nm$ (see figures 7a and 7b) ($D/a = 0.3$ and 0.5, where D is the diameter of NW), we obtain a feature peaked at 850 nm, similar to that reported in GaAs NWs for $D/a \geq 0.13$ [24]. We show in figure 8 (a and b) the reflectance for s- and p- polarized light for $a =$ 100 nm, 200 nm and 300 nm with fixed radius $R = 25\ nm$ and length $h =$ 1000 nm when the incident angle is 30°. We obtain that the reflectance values for all pitch investigated are higher for s-polarization and smaller for p-polarization compared with normal incidence, as we obtained above for the reflectance dependence on radius for oblique incidence. Also, an increasing angle of incidence seems to entail a small number of oscillations of reflectance for all pitch investigated. This phenomenon is consistent with the reduction of oscillations number for all radii investigated when the incident angle is higher. In fact, when the incident angle increases, the light detects less centers of scattering (GaAs NWs) and the number of oscillations in the reflectance is small, independently of the radius and the pitch. In addition, the number of oscillations increases for greater pitch, similar to the case of normal incidence. We obtain an approximate law for the peak-to-peak distance versus a as (4.18 - 0.02 a + $3.21\times10^{-5}a^2$). Our simulations also show a red–shift of the maxima peak position with an approximate law of (4.1 - 0.004 a + $5.7\times10^{-6}a^2$). Although it is not shown here, we obtain

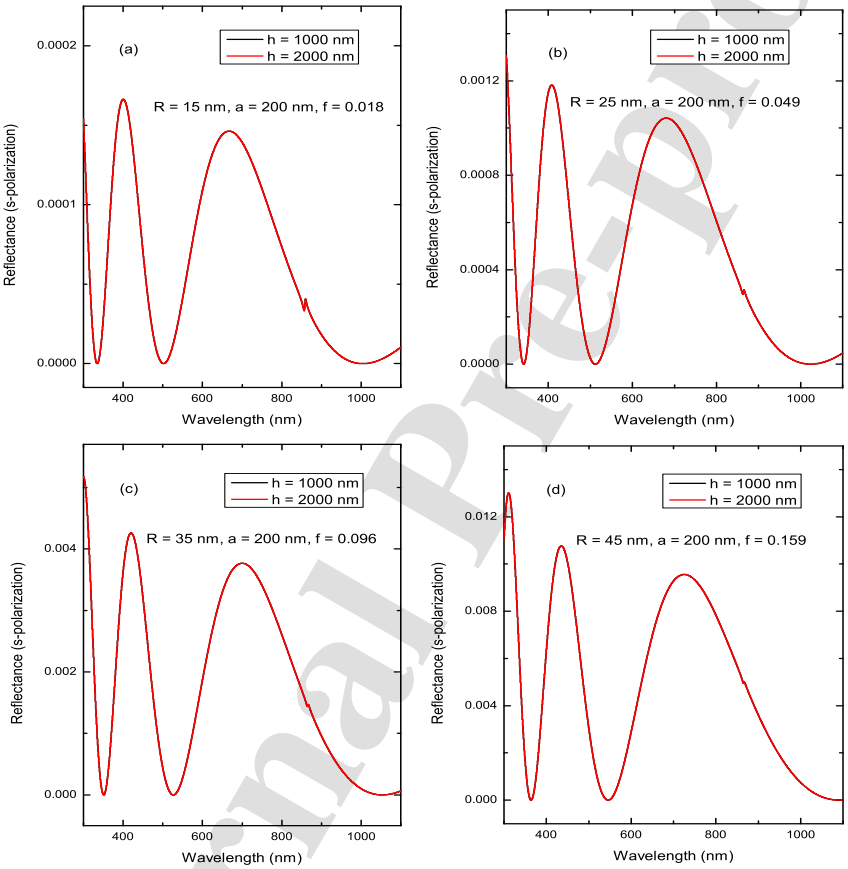

Figure 6: *Reflectance for s-polarized light of the GaAs NWs array for angle of incidence $\theta = 0^o$, pitch a = 200 nm and with length 1000 nm and 2000 nm for different radii (a) R = 15 nm, (b) R = 25 nm, (c) R = 35 nm and (d) R = 45 nm.*

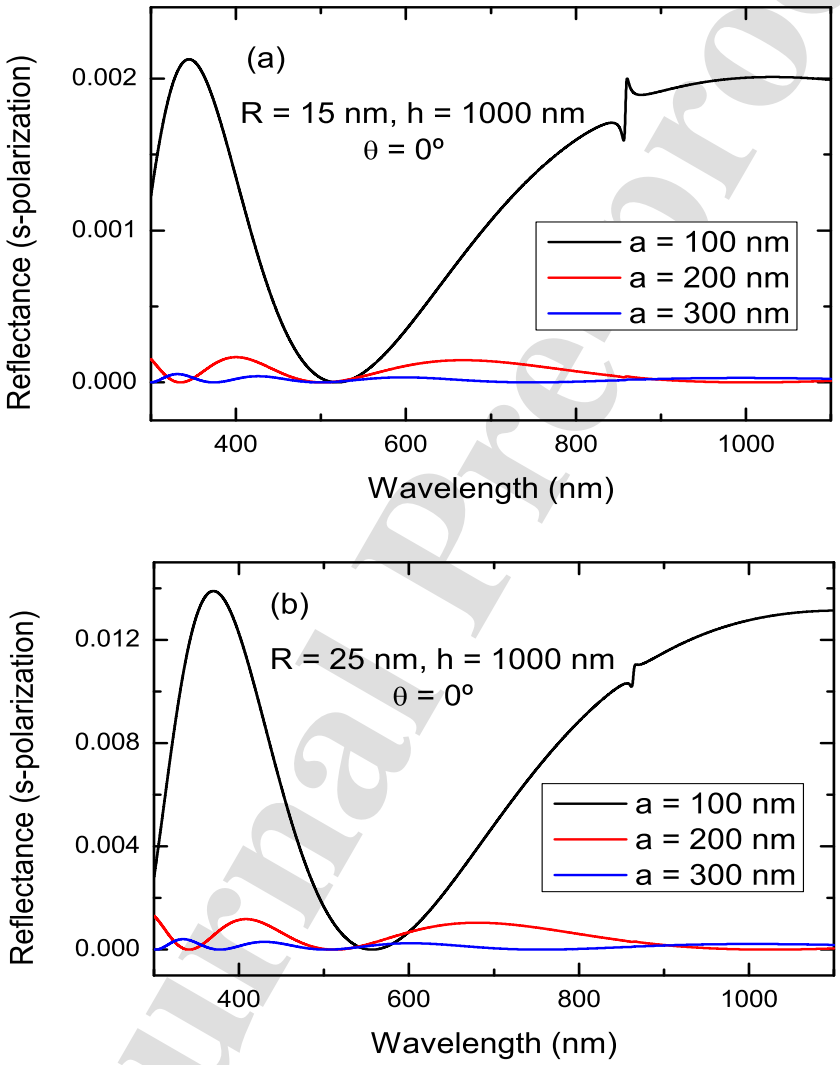

Figure 7: *Reflectance for s-polarized light of the GaAs NWs array for angle of incidence θ = 0° and with pitch 100 nm, 200 nm and 300 nm for (a) R = 15 nm, h = 1000 nm and (b) R = 25 nm, h = 1000 nm.*

that the reflectance dependence on the pitch for higher angles of oblique incidence follows a similar tendency that the case of $\theta = 30^{o}$. In fact, for higher incident angles, the reflectance for s-polarized light is higher compared with the p-polarized light. From the above results, we deduce that the radius and the pitch are relevant parameters to simulate the reflectance in GaAs NWs array at normal and oblique incidences. In fact, there are optimal structural geometrical values, where the GaAs NWs reflectance diminishes. This reduction of reflectance can entail plausible applications in photovoltaic solar cells and waveguides. On the other hand, the simulations with effective medium theory seem to be in good agreement with that reported in the literature using FDTD method in the range of structural values investigated.

4. Conclusion

We have calculated the geometrical effects on the optical reflectance of GaAs NWs array based on transfer matrix formalism and Maxwell–Garnett model. Simulations are performed for s- and p-polarized light. The election of 9 bilayers is motivated for the good approximation to simulate the reflectance spectra. An oscillating behavior of the reflectance is found for both cases, similar to that reported in the literature for other periodical systems. We found that the cylinder's radius and the array's pitch significantly affect the optical reflectance of NWs array. For higher radius, the number of oscillations increases and consequently, the peak-to-peak distance decreases. Besides, there is a red–shift of the reflectance for increasing radius. For higher pitch, the number of oscillations also increases and a red–shift of the reflectance is observed. We obtain dependence laws for the peak-to-peak distance and red–shift versus radius and versus pitch. These dependences obey approximate quadratic relations. Attending to the reflectance dependence on the incident angle, we have found that for s-polarized light, the reflectance is higher for increasing angles, conversely to the case of p-polarized light. In fact, the reflectance values for p-polarization are 2 times lower than the reflectance values of s-polarization for $\theta = 30^{o}$. Therefore, to obtain smaller reflectance values, it is suitable to use non–zero incidence in p-polarization where the reflectance intensity is seen to be better that of s-polarization. However, in normal incidence, both s- and p-polarizations are equivalent. The simulations with effective medium theory and transfer matrix method seem to be in good agreement with that reported in the literature using simulations with FDTD method in the range of structural values investigated.

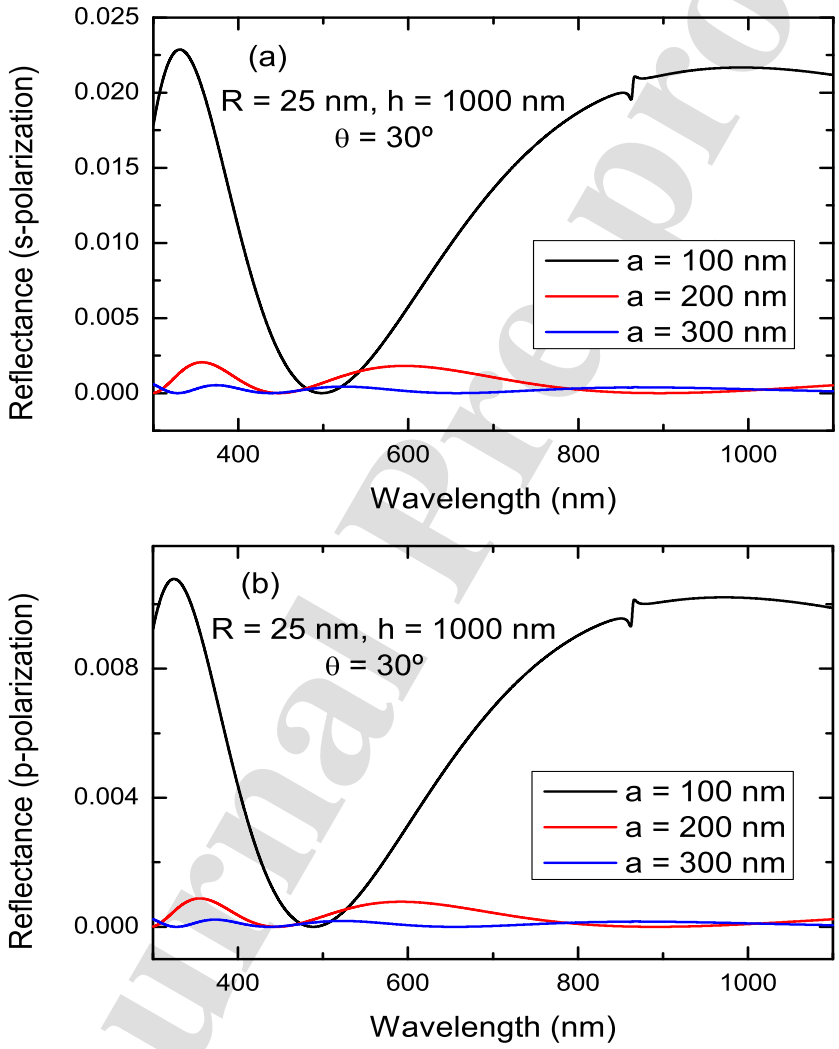

Figure 8: *Reflectance for s- (a) and p- (b) polarized light of the GaAs NWs array for angle of incidence $\theta = 30^{o}$ and with pitch 100 nm, 200 nm and 300 nm. The radius of the NWs is 25 nm and the length is 1000 nm.*

From the above successful results, which combine quantum and effective dielectric theories, we focus in a future work on the influence of the embedding medium along with the composition (band gap energy) on the reflectance of the III-V semiconductors. These features could be relevant in the evaluation of reflectance and absorption in semiconductor NWs. Finally, we propose that our numerical results could insight light for later reflectance measurements in semiconductor NWs array confirming the existence of optimal geometrical parameter values to reduce reflectance. In fact, an estimation of the oscillations number with radius and pitch is obtained.

Credit authorship contribution statment

R.M. de la Cruz: performed simulations, implement the Mathematica and analyzed the results. **C. Kanyinda-Malu:** supervised the computing calculations. **J.E. Muñoz Santiuste:** provided fundings. All the authors contributed to the discussion of data and the writing and editing of the manuscript.

Funding sources

This work is partially supported by Spanish MICINN under grant RTI 2018-101020-B-I00 and TECHNOFUSION III CM–S2018IEMAT–4437. This work has also been supported by Comunidad de Madrid under the agreement with UC3M in the line of Excellence of University Professors (EPUC3M14).

References

[1] J.-J. Chao, S.-C. Shiu, S.-C. Hung and C.-F. Lin C-F, Nanotechnology **21** (2010) 285203.

[2] G. Mariani, A.C. Scofield, C.-H. Hung and D.L. Huffaker, Nat. Commun. **4** (2013) 1497.

[3] M. Tchernycheva et al., Nanotechnology **23** (2013) 265402.

[4] B. Hua, J. Motohisa, Y. Kobayashi, S. Hara and T. Fukui, Nano Lett. **9** (2009) 1126.

[5] D. Saxena, S. Mokkapati, P. Parkinson, N. Jiang, Q. Gao, H.H. Tan and C. Jagadish, Nat. Photonics **7** (2013) 9638.

[6] K. Tomioka, J. Motohisa, S. Hara, K. Hiruma and T. Fukui, Nano Lett. **10** (2010) 163944.

[7] G. Signorello, S. Karg, M.T. Björk, B. Gotsmann and H. Riel, Nano Lett. **13** (2013) 91724.

[8] B. Ganjipour, J. Wallentin, M.T. Borgström, L. Samuelson and C. Thelander, ACS Nano **6** (2012) 310913.

[9] I. Marasovic, T. Garma and T. Betti, J. Phys. D: Appl. Phys. **45** (2012) 215103.

[10] N. Dhindsa, R. Kohandani and S.S. Saini, Nanotechnology **31** (2020) 224001.

[11] L. Cao, J.S. White, J.-S. Park, J.A. Schuller, B.M. Clemens, M.L. Brongersma, Nat. Mater. **8** (2009) 643-647.

[12] L. Cao, P. Fan, A.P. Vasudev, J.S. White, Z. Yu, W. Cai, J.A. Schuller, S. Fan, M.L. Brongersma, Nano Lett. **10** (2010) 439-445.

[13] P.M. Wu, N. Anttu, H.Q. Xu, L. Samuelson, M.E. Pistol, Nano Lett. **12** (2012) 1990-1995.

[14] S.K. Kim, R.W. Day, J. F. Cahoon, T.J. Kempa, K.D. Song, H.G. Park, C.M. Lieber, Nano Lett. **12** (2012) 4971-4976.

[15] J. Svensson, N. Anttu, N. Vainorius, B.M. Borg, L.E. Wernersson, Nano Lett. **13** (2013) 1380-1385.

[16] Y. Huang, T.W. Kim, S. Xiong, L.J. Mawst, T.F. Kuech, P.F. Nealey, Y. Dai, Z. Wang, W. Guo, D. Forbes, S.M. Hubbard, M. Nesnidal, Nano Lett. **13** (2013) 5979-5984.

[17] G. Otnes and M.T. Borgström, Nano Today **12** (2017), 31-45.

[18] N. Dhindsa, A. Chia, J. Boulanger, I. Khodadad, R. LaPierre and S.S. Saini, Nanotechnology **25** (2014) 305303-11.

[19] K.M. Azizur–Rahmanand R.R. LaPierre, Nanotechnology **26** (2015) 295202-7.

[20] A.C. Lesina, A. Vaccari, P. Berini and L. Ramunno, Optics Express **23** (2015) 10481.

[21] T.W. Hertel, IEEE Transactions on antennas and propagation **51** (2003) 1771.

[22] D.E. Aspnes, J.B. Theeten and F. Hotier, Phys. Rev. B **20** (1979) 3292.

[23] T.W.H. Oates and E. Christalle, J. Phys. Chem. C **111** (2007) 182.

[24] R.M. de la Cruz, C. Kanyinda–Malu and J.E. Muñoz Santiuste, Physica B **619** (2021) 413233-7.

[25] N.M. Ali and N.H. Rafat, Renewable and Sustainable Energy Reviews **68** (2017) 212 and references herein.

[26] J.C. Maxwell Garnett, Trans. of the Royal Society, (1904) v. CCIII 385.

[27] K.J. Webb and A. Ludwig, Phys. Rev. B **78** (2008) 153303.

[28] N. Dhindsa and S.S. Saini, Nanotechnology **28** (2017) 235301-9.

[29] F. Floris, L. Fornasari, A. Marini, V. Bellani, F. Banfi, S. Roddaro, D. Ercolani, M. Rocci, F. Beltram, M. Cecchini, L. Sorba and F. Rossella, Nanomaterials **7** (2017) 400; doi:10.3390/nano7110400.

[30] G.Y. Slepyan, S.A. Maksimenko, V.P. Kalosha, J. Herrmann, N.N. Ledentsov, I.L. Krestnikov, Z.I. Alferoz and D. Bimberg, Phys. Rev. B **19** (1999) 12275.

[31] R. Starko-Bowes, J. Atkinson, W. Newman, H. Hu, T. Kallos, G. Palikaras, R. Fedosejevs, S. Pramanik and Z. Jacob, J. Of the Optical Society of America B **32** (2015) 2074.

[32] L.K. van Vugt, Thesis: Optical properties of semiconducting nanowires, www.phys.uu.nl/-vugt.

[33] J.M. Cabrera, F. Agulló and F.J. López, Optica electromagnética, Vol. II: Materiales y aplicaciones, Addison Wesley Iberoamericana Española 2000.

[34] D.Sikdar and A.A. Kornyshev, Scientific Reports 33712, doi:10.1038/srep33712(2016) www.nature.com/scientificreports.

[35] A. Najar, J. Charrier, P. Pirasteh and R. Sougrat, Optics Express **20** (2012) 16861.

[36] A. Gu, Y. Huo, S. Hu. . Sarmiento, E. Picket, D. Liang, S. Li, A. Liu, S. Thombare, Z. Yu, S. Fan, P. McIntyre, Y. Cui and J. Harris, IEEE 978-1-4244-5892-9 (002034) (2010).

[37] Y. Chen, O. Höhn, N. Tucher, M.-E. Pistol and N. Anttu, Optics Express **25** (2017) 294641.

[38] S.L. Diedenhofen, O.T.A. Janssen, G. Grzela, E.P.A.M. Bakkers and J. Gómez Rivas, ACS Nano **5** (2011) 2316.

[39] T.U. Tumkur, J.K. Tikur, B. Chu, L. Gus and V.A. Podolskiy (2012), Birch and NCN Publications Paper 1146, http://dx.doi.org/10.1063/1.4746387.

[40] H. Bao, X. Ruan and T.S. Fisher, Optics Express **18** (2010) 6347.

[41] N. Anttu, V. Dagyté, X. Zeng, G. Otnes and M. Borgström, Nanotechnology **28** (2017) 205203-6.

[42] N. Anttu, A. Abrand, D. Asoli, M. Heurlin, I. Aberg, L. Samuelson and M. Borgström, Nano Research **7** (2014) 816.

[43] M.A. Noginov, H. Li, Yu.A. Barnakov, D. Dryden, G. Nataraj, G. Zhu, C.E. Bonnev, M. Mayy, Z. Jacob and E.E. Narimanov, Optics Lett. **35** (2010) 1863.

[44] P. Yu, S. Liu, J. Xiong, C. Jagadish and Z.M. Wang, Nano Today **11** (2016) 704.

Highlights:

- The structural geometric parameters effects on the reflectance of GaAs nanowires array are investigated.
- The Maxwell-Garnett theory is used to calculate the dielectric function of the GaAs nanowires arrays.
- The transfer matrix formalism is used to analyze the optical reflectance for s- and p-polarized light.
- Among the three parameters considered, nanowire radius and the array pitch are found to be relevant in determining the reflectance at normal and oblique incidences.
- For higher radius and pitch, the number of oscillations of reflectance increase and peaks red-shift are obtained.

Credit Author Statment

R.M. de la Cruz: performed simulations, implement the Mathematica and analyzed the results.

C. Kanyinda-Malu: supervised the computing calculations. **J.E. Muñoz-Santiuste:** provided fundings. All the authors contributed to the discussion of data and the writing and editing of manuscript.

Declaration of interests

☒ The authors declare that they have no known competing financial interests or personal relationships that could have appeared to influence the work reported in this paper.

☐ The authors declare the following financial interests/personal relationships which may be considered as potential competing interests: